
Supplementary information

A cross-platform approach identifies genetic regulators of human metabolism and health

In the format provided by the authors and unedited

Supplementary Material

A cross-platform approach identifies genetic regulators of human metabolism and health

Luca A. Lotta^{1#}, Maik Pietzner^{1#}, Isobel D. Stewart¹, Laura B.L. Wittmans^{1,2}, Chen Li¹, Roberto Bonelli^{3,4}, Johannes Raffler⁵, Emma K. Biggs⁶, Clare Oliver-Williams^{7,8}, Victoria P.W. Auyeung¹, Jian'an Luan¹, Eleanor Wheeler¹, Ellie Paige⁹, Praveen Surendran^{7,10,11,12}, Gregory A. Michelotti¹³, Robert A. Scott¹, Stephen Burgess^{14,15}, Verena Zuber^{14,16}, Eleanor Sanderson¹⁷, Albert Koulman^{1,5,18}, Fumiaki Imamura¹, Nita G. Forouhi¹, Kay-Tee Khaw¹⁵, MacTel Consortium, Julian L. Griffin¹⁹, Angela M. Wood^{7,10,11,20,21}, Gabi Kastenmüller⁵, John Danesh^{7,10,11,20,22,23}, Adam S. Butterworth^{7,10,11,20,22,23}, Fiona M. Gribble⁶, Frank Reimann⁶, Melanie Bahlo^{3,4}, Eric Fauman²⁴, Nicholas J. Wareham¹, Claudia Langenberg^{1,11,25*}

these authors contributed equally

- 1) MRC Epidemiology Unit, University of Cambridge, Cambridge, UK
- 2) The Big Data Institute, Li Ka Shing Centre for Health Information and Discovery, University of Oxford
- 3) Population Health and Immunity Division, The Walter and Eliza Hall Institute of Medical Research, Parkville, Australia
- 4) Department of Medical Biology, The University of Melbourne, Parkville, Australia
- 5) Institute of Computational Biology, Helmholtz Zentrum München – German Research Center for Environmental Health, Neuherberg, Germany
- 6) Metabolic Research Laboratories, University of Cambridge, Cambridge, United Kingdom
- 7) British Heart Foundation Cardiovascular Epidemiology Unit, Department of Public Health and Primary Care, University of Cambridge, Cambridge, UK
- 8) Homerton College, University of Cambridge, Cambridge, UK
- 9) National Centre for Epidemiology and Population Health, The Australian National University, Canberra, Australia
- 10) British Heart Foundation Centre of Research Excellence, University of Cambridge, Cambridge, UK
- 11) Health Data Research UK Cambridge, Wellcome Genome Campus and University of Cambridge, Cambridge, UK
- 12) Rutherford Fund Fellow, Department of Public Health and Primary Care, University of Cambridge, UK
- 13) Metabolon Inc, Durham, North Carolina USA
- 14) MRC Biostatistics Unit, University of Cambridge, Cambridge, United Kingdom
- 15) Department of Public Health and Primary Care, University of Cambridge, Cambridge, United Kingdom
- 16) Department of Epidemiology and Biostatistics, Imperial College London, UK
- 17) MRC Integrative Epidemiology Unit, Bristol Medical School, University of Bristol, UK
- 18) NIHR BRC Nutritional Biomarker Laboratory, University of Cambridge, UK
- 19) Biomolecular Medicine, Department of Metabolism, Digestion and Reproduction, Imperial College London, UK
- 20) National Institute for Health Research Blood and Transplant Research Unit in Donor Health and Genomics, University of Cambridge, Cambridge, UK
- 21) The Alan Turing Institute, London, UK
- 22) National Institute for Health Research Cambridge Biomedical Research Centre, University of Cambridge and Cambridge University Hospitals, Cambridge, UK
- 23) Department of Human Genetics, Wellcome Sanger Institute, Hinxton, UK
- 24) Internal Medicine Research Unit, Pfizer Worldwide Research, Cambridge, MA 02142, USA
- 25) Computational Medicine, Berlin Institute of Health (BIH), Charité University Medicine, Germany

*Corresponding author:

Claudia Langenberg

MRC Epidemiology Unit

University of Cambridge School of Clinical Medicine

Institute of Metabolic Science

Cambridge, UK

claudia.langenberg@mrc-epid.cam.ac.uk

METHODS

Cohort Description

The Fenland study is a population-based cohort study of 12,435 participants without diabetes born between 1950 and 1975¹. Participants were recruited from general practice surgeries in Cambridge, Ely and Wisbech (United Kingdom) and underwent detailed metabolic phenotyping and genome-wide genotyping. Ethical approval for the Fenland study was given by the Cambridge Local Ethics committee (ref. 04/Q0108/19) and all participants gave their written consent prior to entering the study. The European Prospective Investigation of Cancer (EPIC)-Norfolk study is a prospective cohort of 25,639 individuals aged between 40 and 79 and living in the county of Norfolk in the United Kingdom at recruitment². The study was approved by the Norfolk Research Ethics Committee (REC ref. 98CN01) and all participants gave their written consent before entering the study. INTERVAL is a randomised trial of approximately 50,000 whole blood donors enrolled from all 25 static centres of NHS Blood and Transplant, aiming to determine whether donation intervals can be safely and acceptably decreased to optimise blood supply whilst maintaining the health of donors³. All participants of the study gave written informed consent and the study was approved by NRES Committee East of England - Cambridge East (ref. 11/EE/0538).

Metabolomics Measurements in Fenland Cohort

We used a Waters Acquity ultra-performance liquid chromatography (UPLC; Waters Ltd, Manchester, UK) system coupled to an ABSciex 5500 Qtrap mass spectrometer (Sciex Ltd, Warrington, UK). Samples were derivatised and extracted using a Hamilton STAR liquid handling station (Hamilton Robotics Ltd, Birmingham, UK). Flow injection analysis coupled with tandem mass spectrometry (FI-MS/MS) using multiple reaction monitoring (MRM) in positive mode ionisation was performed to measure the relative levels of acylcarnitines, phosphatidylcholines, lysophosphatidylcholines and sphingolipids. The level of hexose was measured in negative ionisation mode. Ultra-performance liquid chromatography coupled with tandem mass spectrometry using MRM was performed to measure the concentration of amino acids and biogenic amines. The chromatography consisted of a 5-minute gradient starting at 100% aqueous (0.2% Formic acid) increasing to 95% acetonitrile (0.2% Formic acid) over a Waters Acquity UPLC BEH C18 column (2.1 x 50 mm, 1.7 µm, with guard column). Isotopically labelled internal standards are integrated within the Biocrates p180 Kit for quantification. Data was processed in the Biocrates Met/DQ software. Raw metabolite readings underwent extensive quality control procedures. Firstly, we excluded from any further analysis

metabolites for which the number of measurements below the limit of quantification (LOQ) exceeded 5% of measured samples. Excluded metabolites were carnosine, dopamine, putrescine, asymmetric dimethyl arginine, dihydroxyphenylalanine, nitrotyrosine, spermine, sphingomyelins SM(22:3), SM(26:0), SM(26:1), SM(24:1-OH), phosphatidylcholine acyl-alky 44:4, and phosphatidylcholine diacyl C30:2. Secondly, in samples with detectable but not quantifiable peaks, we assigned random values between 0 and the run-specific LOQ of a given metabolite. Finally, we corrected for batch-effects with a “location-scale” approach, i.e. with normalization for mean and standard deviation of batches.

The Metabolon HD4 platform (EPIC-Norfolk and INTERVAL)

For these measurements, instrument variability, determined by calculating the median relative standard deviation, was of 6%. Data Extraction and Compound Identification: raw data was extracted, peak-identified and quality control-processed using Metabolon’s hardware and software. Compounds were identified by comparison to library entries of purified standards or recurrent unknown entities. Metabolon maintains a library, based upon authenticated standards, that contains the retention time/index (RI), mass to charge ratio (m/z), and chromatographic data (including MS/MS spectral data) of all molecules present in the library. Identifications were based on three criteria: retention index, accurate mass match to the library +/- 10 ppm, and the MS/MS forward and reverse scores between the experimental data and authentic standards. Metabolite Quantification and Data Normalization: Peaks were quantified using area-under-the-curve. A data normalization step was performed to correct variation resulting from instrument inter-day tuning differences. Essentially, each compound was corrected in run-day blocks by registering the medians to equal one (1.00) and normalizing each data point proportionately (termed the “block correction”).

The Nightingale platform (INTERVAL)

The serum levels of 230 metabolites were measured in the INTERVAL study using ¹H-NMR spectroscopy^{4,5}. Among those, 10 metabolites (creatinine, alanine, glutamine, glycine, histidine, isoleucine, leucine, valine, phenylalanine, and tyrosine) overlapped with what is captured by the Biocrates p180 Kit and were used in the present study. Further details of the ¹H-NMR spectroscopy, quantification data analysis and identification of the metabolites have been described previously^{5,6}. Participants with >30% of metabolite measures missing and duplicated individuals were removed. Metabolite data more than 10 SD from the mean was also removed.

GWAS analysis

Genotyping in Fenland was done in two waves including 1,500 (Affymetrix SNP5.0) and 9,369 (Affymetrix Axiom) participants and imputation was done using IMPUTE2 to 1000 Genomes Phase 1v3 (Affymetrix SNP5.0) or phase 3 (Affymetrix Axiom) reference panels (**Supplemental Tab. S1**). Plasma metabolite and genotype data was available for 8,714 (Affymetrix Axiom) and 1,022 (Affymetrix SNP5.0) unrelated individuals. In EPIC-Norfolk, 21,044 samples were forwarded to imputation using 1000 Genomes Phase 3 (Oct. 2014) reference panels (**Supplemental Tab. S1**). Imputed SNPs with imputation quality score less than 0.3 or minor allele account less than 2 were removed from the imputed dataset. Genome-wide association analyses were carried out using BOLT-LMM v2.2 adjusting for age, sex, and study-specific covariates in mixed linear models. Alternatively (when the BOLT-LMM algorithm failed due to heritability estimates close to zero or one) analyses were performed using SNPTEST v2.4.1 in linear regression models, additionally adjusting for the top 4 genetic ancestry principal components and excluding related individuals (defined by proportion identity-by-descent calculated in Plink⁷ > 0.1875 as recommended⁸). GWAS analyses in Fenland were performed within genotyping chip, and associations meta-analysed.

In INTERVAL, genotyping was conducted using the Affymetrix Axiom genotyping array. Standard quality control procedures were conducted prior to imputation. The data were phased and imputed to a joint 1000 Genomes Phase 3 (May 2013)-UK10K reference imputation panel. After QC, a total of 40,905 participant remained with data obtained by ¹H-NMR spectroscopy. For variants with a MAF of >1% and imputed variants with an info score of >0.4 a univariate GWAS for each of the ten metabolic measures was conducted, after adjustment for technical and seasonal effects, including age, sex, and the first 10 principal components, and rank-based inverse normal transformation. The association analyses were performed using BOLT-LMM v2.2 and R. Data based on the Metabolon HD4 platform was available for 8,455 participants. Prior to the Metabolon HD4 genetic analysis, genetic data were filtered to include only variants with a MAF of >0.01% and imputed variants with an info score of >0.3. Phenotype residuals corrected for age, gender, metabolon batch, INTERVAL centre, plate number, appointment month, the lag time between the blood donation appointment and sample processing, and the first 5 ancestry principal components were calculated for each metabolite and the residuals were standardised prior to the genetic analyses in SNPTEST v2.5.1.

For all GWAS analysis within Fenland, EPIC-Norfolk and INTERVAL, variants with Hardy-Weinberg equilibrium $p < 1 \times 10^{-6}$ and associations with absolute value of effect size >5 or standard error (SE) >10 or <0 were excluded; insertions and deletions were excluded.

Investigation of heterogeneity

We used a meta-regression model to identify factors associated with larger I^2 values across all 499 identified SNP-metabolite associations. To this end, a vector of heterogeneity estimates, I^2 , from the meta-analysis was obtained as outcome and the following explanatory variables were considered: strength of effect (absolute Z-score of the SNP – metabolite association), biochemical class, dummy variables indicating the study of origin (related to the measurement platform), and the number of contributing studies as an estimate of sample size. A significant effect of any of those terms in a linear regression model was taken to indicate a source of heterogeneity across SNP-metabolite associations and hence identified systematic factors contributing to any observed cross-platform heterogeneity.

Conditional analysis

We tested at each locus for conditional independent variants using exact stepwise conditional analysis in the largest Fenland sample ($n = 8,714$) using SNPTTEST v2.5 with the same baseline adjustment as in the discovery approach. To refine signals at those loci we used a more recent imputation for this analysis based on the HRC v1 reference panel and additional SNPs imputed using UK10K and 1000G phase 3. We defined secondary signals as those with a conditional p-value $< 5 \times 10^{-8}$. To avoid problems with collinearity we tested after each round if inclusion of a new variant changed associations of all previous variants with the outcome using a joint model. If this model indicated that one or more of the previously selected variants dropped below the applied significance threshold we stopped the procedure, otherwise we repeated this procedure until no further variant met the significance threshold in conditional models. We considered only locus-metabolite associations meeting the GWAS-threshold for significance in the Fenland analysis ($n=228$).

Statistical fine-mapping

Regional summary statistics (betas and standard errors) were converted to approximate Bayes factors as described in Wakefield *et al.*⁹ to calculate the posterior probability (PP) for each variant driving the association. Credible sets are subsequently defined as the ranked list of variants cumulatively covering 99% of the PP to cover the true causal signal. For loci with evidence of independent secondary signals we used GCTA COJO-cond algorithm to generate conditional association statistics conditioning on all other independent signals in the locus. Since the calculation of approximate Bayes factors requires betas and standard errors we used meta-analysis results across studies for which we had access to individual data (Fenland, EPIC-Norfolk, and INTERVAL).

However, out of 546 detected signals 473 reached genome-wide significance ($p < 5 \times 10^{-8}$) in this smaller subset and we restricted fine-mapping to those associations.

Knowledge-based (biological) assignment of causal genes

The following seven sources have been used to assign potential causal genes based on curated databases.

- 1) HMDB metabolite names¹⁰ were compared to each Entrez gene name;
- 2) Metabolite names were compared to the name and synonyms of the protein encoded by each gene¹¹
- 3) HMDB metabolite names and their parent terms (class) were compared to the names for the protein encoded by each gene (UniProt).
- 4) Metabolite names were compared to rare diseases linked to each gene in OMIM¹² after removing the following non-specific substrings from disease names: uria, emia, deficiency, disease, transient, neonatal, hyper, hypo, defect, syndrome, familial, autosomal, dominant, recessive, benign, infantile, hereditary, congenital, early-onset, idiopathic;
- 5) HMDB metabolite names and their parent terms were compared to all GO biological processes associated with each gene after removing the following non-specific substrings from the name of the biological process: metabolic process, metabolism, catabolic process, response to, positive regulation of, negative regulation of, regulation of. For this analysis only gene sets containing fewer than 500 gene annotations were retained.
- 6) KEGG maps¹³ containing the metabolite as defined in HMDB were compared to KEGG maps containing each gene, as defined in KEGG. For this analysis the large “metabolic process” map was omitted.
- 7) Each proximal gene was compared to the list of known interacting genes as defined in HMDB.

Multi-trait colocalisation across metabolites

We used hypothesis prioritisation in multi-trait colocalisation (HyPrColoc)¹⁴ at each of the identified 144 loci 1) to identify metabolites sharing a common causal variant over and above what could be identified in the meta-analysis to increase statistical power, and 2) to identify loci with evidence of multiple causal variants with distinct associated metabolite clusters. HyPrColoc provides for each cluster three different types of output: 1) a posterior probability (PP) that all traits in the cluster share a common genetic signal, 2) a regional association probability, i.e. that all the

metabolites share an association with one or more variants in the region, and 3) the proportion of the PP explained by the candidate variant. We considered a highly likely alignment of a genetic signal across various traits if the PP > 75% or the regional association probability > 80% and the PP > 50%. The second criterion takes into account that metabolites may share multiple causal variants at the same locus. We used the same set of summary statistics as described for statistical fine-mapping. We further filtered metabolites with no evidence of a likely genetic signal ($p > 10^{-5}$) in a region before performing HyPrColoc, which improved clustering across traits by minimizing noise. We used the same workflow to test for the alignment of a genetic signal at the *GLPR2* locus using summary statistics from T2D (see below), a meta-analysis for body mass index across GIANT and UK Biobank, plasma GIP, and plasma citrulline.

Enrichment of type 2 diabetes associations among metabolite associated lead variants

We examined whether the set of independent lead metabolite associated variants (N=168) were enriched for associations with T2D. We plotted observed versus expected $-\log_{10}(p\text{-values})$ for the 168 lead variants in a QQ-plot, using association statistics from a T2D meta-analysis including 80,983 cases and 842,909 non-cases from the DIAMANTE study¹⁵ (55,005 T2D cases, 400,308 non-cases), UK Biobank¹⁶ (24,758 T2D cases, 424,575 non-cases, application number 44448) and the EPIC-Norfolk study (additional T2D cases not included in DIAMANTE study: 1,220 T2D cases and 18,026 non-cases). This QQ-plot was compared to those for 1000 sets of variants, where variants in each set were matched to the index metabolite variants in terms of MAF, the number of variants in LD ($R^2 > 0.5$), gene density and distance to nearest gene (for all parameters $\pm 50\%$ of the index variant value), but otherwise randomly sampled from across the autosome excluding the HLA region. MAF and LD parameters for individual variants were determined from the EPIC-Norfolk study (using the combined HRC, UK10K and 1000G imputation as previously described) and gene information was derived from GENCODE v19 annotation¹⁷. A one-tailed Wilcoxon rank sum test was used to compare the distribution of association $-\log_{10} p$ -values for the metabolite associated variants with that for the randomly sampled, matched, variants.

1. Lindsay, T. *et al.* Descriptive epidemiology of physical activity energy expenditure in UK adults (The Fenland study). *Int. J. Behav. Nutr. Phys. Act.* **16**, 126 (2019).
2. Day, N. *et al.* EPIC-Norfolk: study design and characteristics of the cohort. European Prospective Investigation of Cancer. *Br. J. Cancer* **80 Suppl 1**, 95–103 (1999).
3. Moore, C. *et al.* The INTERVAL trial to determine whether intervals between blood donations can be safely and acceptably decreased to optimise blood supply: Study protocol for a randomised controlled trial. *Trials* **15**, (2014).

4. Di Angelantonio, E. *et al.* Efficiency and safety of varying the frequency of whole blood donation (INTERVAL): a randomised trial of 45 000 donors. *Lancet* **390**, 2360–2371 (2017).
5. Soininen, P. *et al.* High-throughput serum NMR metabonomics for cost-effective holistic studies on systemic metabolism. *Analyst* **134**, 1781–5 (2009).
6. Inouye, M. *et al.* Metabonomic, transcriptomic, and genomic variation of a population cohort. *Mol. Syst. Biol.* **6**, 441 (2010).
7. Purcell, S. *et al.* PLINK: A tool set for whole-genome association and population-based linkage analyses. *Am. J. Hum. Genet.* **81**, 559–575 (2007).
8. Anderson, C. A. *et al.* Data quality control in genetic case-control association studies. *Nat. Protoc.* **5**, 1564–1573 (2011).
9. Wakefield, J. Bayes Factors for Genome-Wide Association Studies : Comparison with P - values. **86**, 79–86 (2009).
10. Wishart, D. S. *et al.* HMDB 4.0: The human metabolome database for 2018. *Nucleic Acids Res.* **46**, D608–D617 (2018).
11. Bateman, A. *et al.* UniProt: The universal protein knowledgebase. *Nucleic Acids Res.* **45**, D158–D169 (2017).
12. Rath, A. *et al.* Representation of rare diseases in health information systems: The orphanet approach to serve a wide range of end users. *Hum. Mutat.* **33**, 803–808 (2012).
13. Kanehisa, M., Furumichi, M., Tanabe, M., Sato, Y. & Morishima, K. KEGG: New perspectives on genomes, pathways, diseases and drugs. *Nucleic Acids Res.* **45**, D353–D361 (2017).
14. Foley, C. N. *et al.* A fast and efficient colocalization algorithm for identifying shared genetic risk factors across multiple traits. **44**, 1–47 (2019).
15. Mahajan, A. *et al.* Fine-mapping type 2 diabetes loci to single-variant resolution using high-density imputation and islet-specific epigenome maps. *Nat. Genet.* **50**, 1505–1513 (2018).
16. Sudlow, C. *et al.* UK Biobank: An Open Access Resource for Identifying the Causes of a Wide Range of Complex Diseases of Middle and Old Age. *PLoS Med.* **12**, (2015).
17. Frankish, A. *et al.* GENCODE reference annotation for the human and mouse genomes. *Nucleic Acids Res.* **47**, D766–D773 (2019).

FIGURES

Figure S1

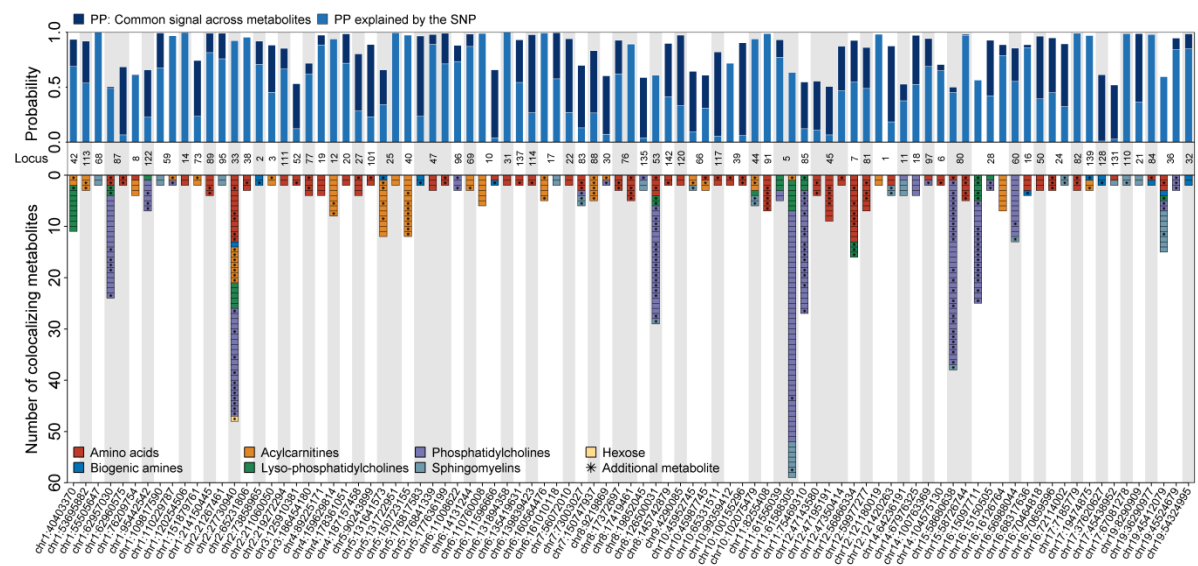


Figure S1 Summary of statistical colocalization analysis across metabolites for 72 loci with evidence (posterior probability >75% or regional probability >80%) for a shared genetic signal across at least two metabolites. The upper panels display the posterior probabilities (PP) for a shared genetic signal across metabolites (dark blue) and the PP explained by the candidate SNP displayed on the x-axis (blue). The lower panel displays the number and class of metabolites sharing a genetic signal. Metabolites discovered using colocalization only, are indicated by stars. The row in the middle refers to the numbering of loci from Supplemental Table S2.

Figure S2

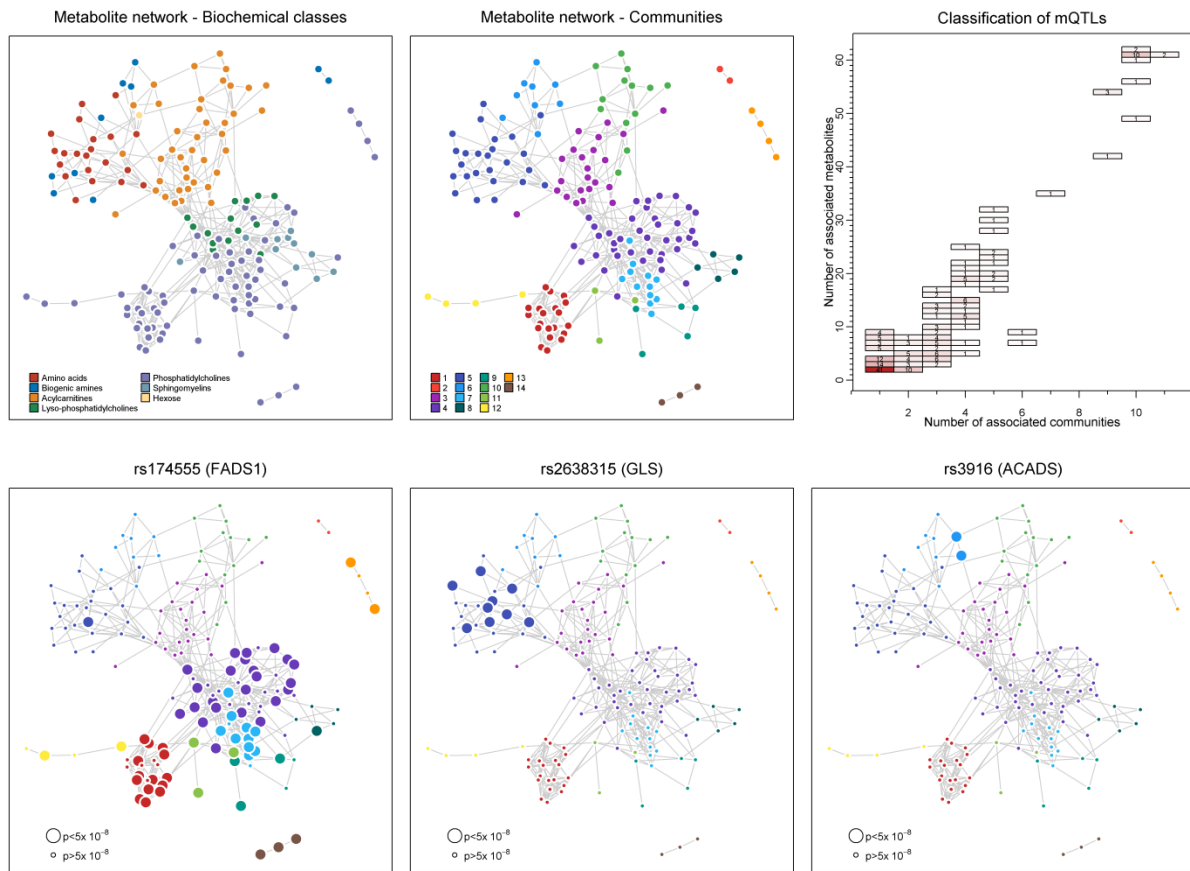


Figure S2 Derived metabolic network from Gaussian graphical modelling. Each edge represents a significant partial correlation between metabolites, i.e. a significant correlation between two metabolites after taking into account all other metabolites in the network. The left and middle plot in the upper panel show the metabolite network coloured by biochemical class versus identified modules/communities, respectively. The right plot in the upper panel shows the number of associated metabolites ($p < 5 \times 10^{-8}$) for each of the 304 metabolite quantitative trait loci against the distribution of those across the number of identified communities. The lower panel maps specific variants onto the network indicating significance by node size.

Figure S3

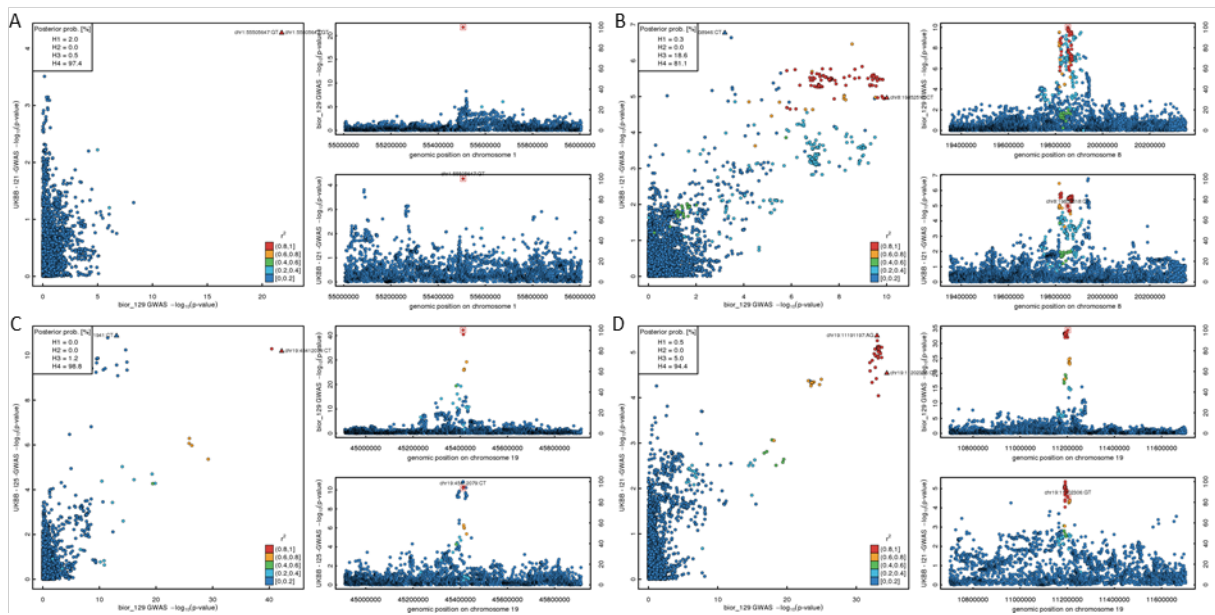


Figure S3. Triplet of plots to compare regional associations profiles for results (p-values on a $-\log_{10}$ scale) from genome-wide association analysis (GWAS) for SM C16:0 (x-axis, *bio129*) and a disease trait from UK Biobank (y-axis, I21 – Acute myocardial infarction, I25 – Chronic ischaemic heart disease) at A) *PCSK9*, B) *LPL*, C) *LDLR*, and D) *APOE*. Regions were chosen based on the purification workflow to reveal links to inborn errors of metabolism (see Main text). The legend displays posterior probabilities from statistical colocalisation analyses on the following hypothesis: H0 – no signal; H1 – signal unique to the metabolite; H2 – signal unique to the trait; H3 – two distinct causal variants in the same locus and H4 – presence of a shared causal variant between a metabolite and a given trait. The strongest variants for each trait in the locus are annotated and LD-based colouring was done with respect to the lead variant.

Figure S4

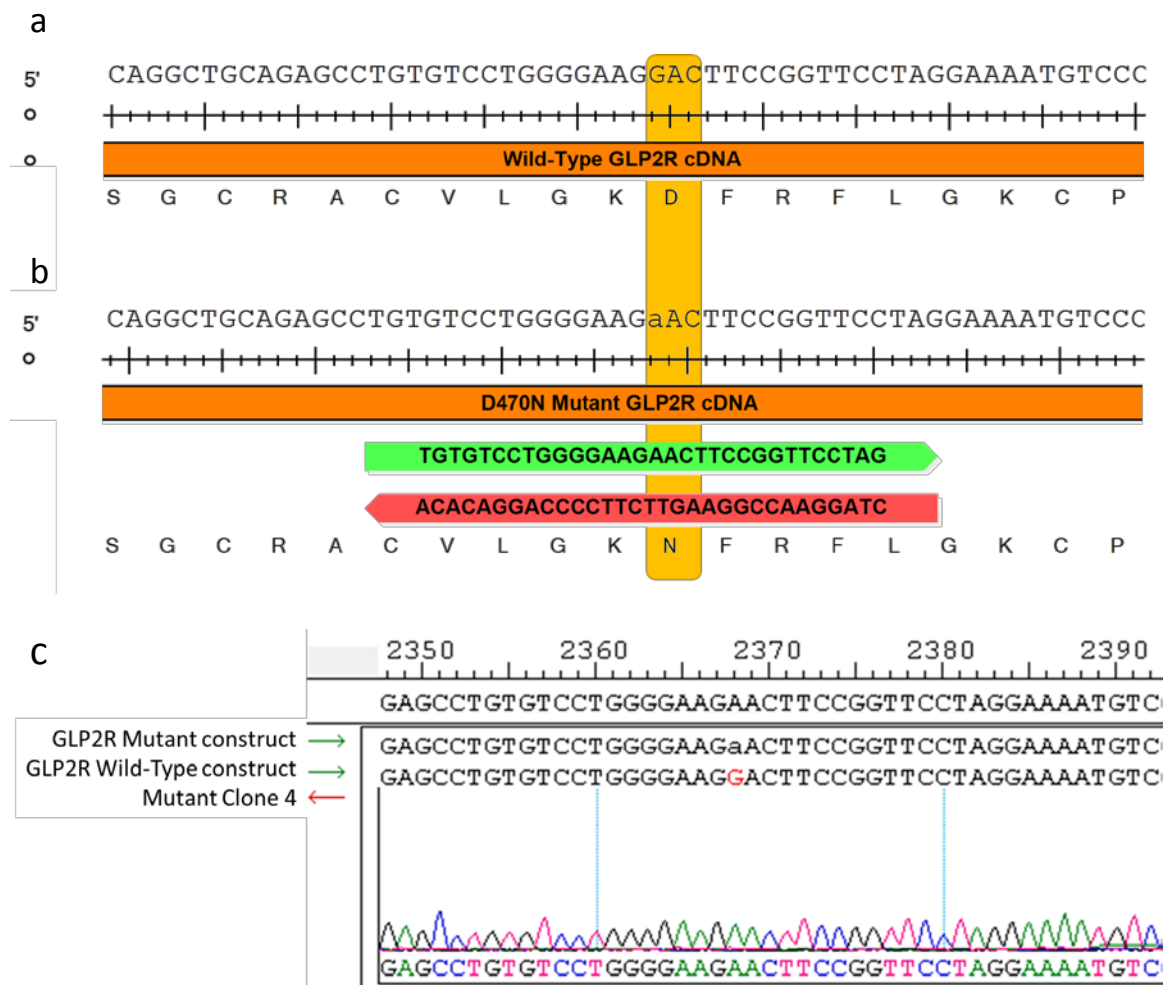


Figure S4. Schematic depicted wild-type and mutant GLP2R sequences. (a) Wild-type GLP2R sequence, amino acid targeted for mutation is highlighted in yellow. (b) Mutant GLP2R sequence, showing D470N mutation highlighted in yellow. Primers used to introduce the mutation using QuikChange Lightning Site-Directed Mutagenesis are depicted, forward primer shown in green, and reverse primer shown in red. (c) Sequence confirmation of successfully mutagenesis, chromatogram depicted for clone 4 which was then sequenced in full.

Figure S5

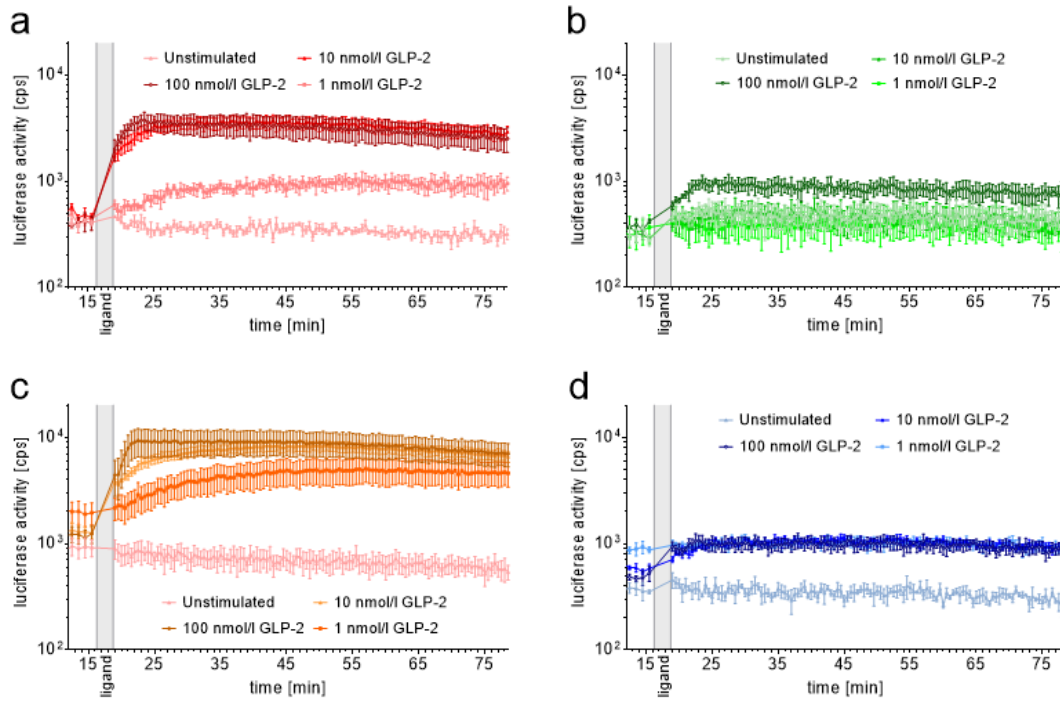


Figure S5. Example traces of GLP2R wild-type and mutant signalling via beta-arrestin 1 and beta-arrestin 2. Example real-time beta arrestin responses to a dose titration of GLP-2 are displayed for beta-arrestin 1 (a, b) for wild-type GLP2R (a) and D470N mutant GLP2R (b). Real time beta arrestin responses are also displayed for beta-arrestin 2 (c, d) for wild-type GLP2R (c) and D470N mutant GLP2R (d). Data are from representative experiments, and are displayed as mean \pm SEM from 3 wells.

Supplementary Note

A cross-platform approach identifies genetic regulators of human metabolism and health

Luca A. Lotta^{1#}, Maik Pietzner^{1#}, Isobel D. Stewart¹, Laura B.L. Wittemans^{1,2}, Chen Li¹, Roberto Bonelli^{3,4}, Johannes Raffler⁵, Emma K. Biggs⁶, Clare Oliver-Williams^{7,8}, Victoria P.W. Auyeung¹, Jian'an Luan¹, Eleanor Wheeler¹, Ellie Paige⁹, Praveen Surendran^{7,10,11,12}, Gregory A. Michelotti¹³, Robert A. Scott¹, Stephen Burgess^{14,15}, Verena Zuber^{14,16}, Eleanor Sanderson¹⁷, Albert Koulman^{1,5,18}, Fumiaki Imamura¹, Nita G. Forouhi¹, Kay-Tee Khaw¹⁵, MacTel Consortium, Julian L. Griffin¹⁹, Angela M. Wood^{7,10,11,20,21}, Gabi Kastenmüller⁵, John Danesh^{7,10,11,20,22,23}, Adam S. Butterworth^{7,10,11,20,22,23}, Fiona M. Gribble⁶, Frank Reimann⁶, Melanie Bahlo^{3,4}, Eric Fauman²⁴, Nicholas J. Wareham¹, Claudia Langenberg^{1,11*}

MacTel Project Consortium

Name	Affiliation
Alain Gaudric, MD	Hôpital Lariboisière, Paris, France
Alexander Brucker, MD	Scheie Eye Institute, Pennsylvania, USA
Amani Fawzi, MD	Northwestern University, Illinois, USA
Arshad Khanani, MD	Sierra Eye Associates Ryland Street, Reno, NV, US
Carel Hoyng, MD	of ophthalmology & human genetics, Nijmegen, Netherlands
Cathy Egan, MD	Moorfields Eye Hospital, London, UK
CB Hoyng, MD	Radboud University Medical Center, Nijmegen, Netherlands
Cecilia Lee, MD	University of Washington Eye Institute, Washington, USA
Charles Wykoff, MD, PhD	Retina Consultants of Houston, Texas, USA
Chirag Jhaveri, MD	Retina Research Center, Texas, USA
Christian Metallo, PhD	University of California, San Diego, CA, US
Daniel Joseph, MD, PhD	The Retina Institute, Missouri, USA
Daniel Miller, MD	Cincinnati Eye Institute, CEI Physicians PSC, Inc. Ohio, USA
Daniel Pauleikhoff, Prof. Dr.	St. Franziskus Hospital, Muenster, Germany
David Boyer, MD	Retina-Vitreous Associates Medical Group, California, USA
David Lally, MD	New England Retina Consultants, PC, Massachusetts, USA
David Warrow, MD	Cumberland Valley Retina Consultants, Maryland, USA
David Weinberg, MD	Medical College of Wisconsin, Wisconsin, USA
Diana Do, MD	Byers Eye Institute – Stanford University, California, USA
Emily Chew, MD	National Eye Institute, Maryland, USA
Felicitas Bucher, MD	Eye Center, Medical Center, Faculty of Medicine, University of Freiburg, Freiburg, Germany
Ferenc Sallo, MD	University of Lausanne, Lausanne, Switzerland
Frank Holz, MD	University of Bonn, Bonn, Germany
Gary Fish, MD	Texas Retina Associates, Texas, USA
Glenn Stoller, MD	Ophthalmic Consultants of Long Island, Oceanside, NY, US
Grant Comer, MD	University of Michigan, Kellogg Eye Center, Ann Arbor, MI, US
Ian Constable, MD	Lions Eye Institute, Nedlands, Australia
Irene Leung, MD	Moorfields Eye Hospital, London, UK
Jacque Duncan, MD	University of California, San Francisco, California, USA
Jawad Qureshi, MD	Retina Center of Texas, Texas, USA
Jean-Pierre Hubschman, MD	Jules Stein Eye Institute, UCLA, California, USA

Jennifer Trombley,	Lowy Medical Research Institute
Jiong Yan, MD	Emory University, Georgia, USA
Joan Miller, MD	Massachusetts Eye and Ear, Massachusetts, USA
Johannes Vingerling,MD	Eramus Department of Ophthalmology, Erasmus medical center, Rotterdam, The netherlands
John A Wells,MD	Palmetto retina center, llc, West columbia, SC, US
Joseph M Googe jr,MD	Southeastern Retina Associates, Knoxville, TN, US
Joseph Moisseiev,MD	The Goldschleger Eye Institute, Tel Hashomer, Israel
Khaled Tawansy,MD	Global Research Foundation, Los Angeles, CA, US
Konstantinos Balaskas,MD, PhD	Moorfields Eye Hospital Reading Centre
Lars Freisberg, MD	Tulsa Retina Consultants, Oklahoma, USA
Lawrence A Yannuzzi,MD	Vitreous, Retina, Macula Consultants of New York, New York, NY, US
Lawrence Singerman, MD	Retina Associates of Cleveland, Inc., Ohio, USA
Marcus Fruttiger,PhD	University College London Institute of Ophthalmology, London, UK
Mark Gillies, MD	Save Sight Institute, Sydney, Australia
Martin Friedlander, MD, PhD	Lowy Medical Research Institute
Melanie Bahlo,PhD	Walter and Eliza Hall Institute of Medical Research
Michael J Elman,MD	Elman retina group, Baltimore, MD, US
Michael Lee, MD	Retina Northwest – Portland, Oregon, USA
Mina Chung,MD	University of Rochester, Rochester, NY, US
Patrick Higgins,MD	Retina center of New Jersey, NJ, US
Paul Bernstein, MD, PhD	University of Utah Health Care, Utah, USA
Paul V Raphaelian,MD	Grand rapids Associated Retinal Consultants, Grand rapids, MI, US
Peter Charbel Issa, MD, DPhil, FEBO	Oxford Eye Hospital, Oxford, UK
Philip Rosenfeld, MD, PhD	Bascom Palmer, Florida, USA
Rando Allikmets, PhD	Columbia University, New York, USA
Richard Hamilton, MD	Center for Retina and Macular Disease – Central Florida, Florida, USA
Robyn Guymer, PhD	Centre for Eye Research, East Melbourne, Australia
Roger Goldberg, MD	Bay Area Retina Associates, California, USA
Ryan Rich, MD	Retina Consultants of Southern Colorado, Colorado, USA
Sandeep Randhawa,MD	Royal Oak Associated Retinal Consultants, Royal oak, MI, US
Sarah Duwel, RN, MA, CCRA	Emmes, Maryland, USA
Scott Sneed,MD	Traverse City Associated Retinal Consultants, Traverse City, MI, US
Sophie Bakri,MD	Mayo clinic, Rochester, MN, US
Stanislav V. Zhuk, MD, FACS	Retina Associates New Orleans, Louisiana, USA
Steve Charles,MD	Charles Retina, Germantown, TN, US
Sunil S Patel,MD, PhD	Retina research institute of Texas, Abilene, TX, US
Traci Clemons, PhD	Emmes, Maryland, USA
Tunde Peto, MD	Queens University Belfast, Belfast, UK
